# EFFICIENT APPROXIMATION OF OPTIMAL TRANSPORTATION MAP BY POGORELOV MAP

Dongsheng An $^1$  Na Lei $^2$  Wei Chen $^2$  Zhongxuan Luo $^2$  Tong Zhao $^3$  Hang Si $^4$  Xianfeng Gu $^1$ 

<sup>1</sup>Stony Brook University, NY, U.S.A. {doan, gu} @cs.stonybrook.edu
<sup>2</sup>Dalian University of Technology, Liaoning, China. {nalei, zxluo} @dlut.edu.cn,
wei.chen@mail.dlut.edu.cn
<sup>3</sup>Université Côte d'Azur, Inria, France. tong.zhao@inria.fr
<sup>4</sup>Weierstrass Institute for Applied Analysis and Stochastics (WIAS), Berlin, Germany. si@wias-berlin.de

#### **ABSTRACT**

Optimal transportation (OT) finds the most economical way to transport one measure to another and plays an important role in geometric modeling and processing. Based on the Brenier theorem, the OT problem is equivalent to the Alexandrov problem, which is the dual to the Pogorelov problem. Although solving the Alexandrov/Pogorelov problem are both equivalent to solving the Monge-Ampère equation, the former requires second type boundary condition and the latter requires much simpler Dirichlet boundary condition. Hence, we propose to use the Pogorelov map to approximate the OT map. The Pogorelov problem can be solved by a convex geometric optimization framework, in which we need to ensure the searching inside the admissible space. In this work, we prove the discrete Alexandrov maximum principle, which gives an apriori estimate of the searching. Our experimental results demonstrate that the Pogorelov map does approximate the OT map well with much more efficient computation.

Keywords: Optimal transport, Monge-Ampère equation, Pogorelov problem, Alexandrov maximum principle

#### 1. INTRODUCTION

Recently, optimal transportation has become one of the fundamental tools in geometric modeling and processing, since it can find the most economical way to transfer one probability measure to another, and measure the Wasserstein distance between the measures. It has been applied for area-preserving parameterizations [1], 3D surface registration and comparison [2], medical image registration [3] and so on. It has been applied broadly in generative models in deep learning, e.g. WGAN [4], where the generator computes the optimal transportation map, and the discriminator calculates the Wasserstein distance. It is also used for reflector and refractor design in optics field [5, 6].

# 1.1 Brenier Problem, Alexandrov Problem and Pogorelov Problem

According to Brenier's theory [7], the optimal transportation map, under the quadratic Euclidean distance cost function, is the gradient map of a convex function, the so-called Brenier potential. The Brenier potential satisfies the Monge-Ampère equation. Recently, [8] point out that the Brenier theorem is equivalent to the classical Alexandrov theorem in convex geometry. The Alexandrov theorem states that a convex polyhedron is fully determined, uniquely up to a vertical translation, by its face normals and face areas. The Alexandrov polyhedron is in fact equivalent to the graph of the Brenier potential. The famous Pogorelov problem can be treated as the Legendre dual to the Alexandrov problem, which claims that a convex poly-

hedron is determined by the discrete curvature at the given points.

The Brenier optimal transportation problem (or equivalently the Alexandrov problem), and the Pogorelov problem are reduced to solving the Monge-Ampère equation with different boundary conditions. Suppose the source measure is  $d\mu = f(x)dx$  with the support  $\Omega \subset \mathbb{R}^d$  and the target measure is  $d\nu = g(y)dy$  with the support  $\Omega^* \in \mathbb{R}^d$ , the Briener potential is  $u: \Omega \to \mathbb{R}$ , which satisfies the Monge-Ampère equation with the second type boundary condition:

$$\det D^2 u = \frac{f(x)}{g \circ \nabla u(x)}, \quad s.t. \nabla u(\Omega) = \Omega^*.$$

We call the solution u to the Pogorelov problem as the Pogorelov potential, its gradient is called the Pogorelov map. The Pogorelov potential also satisfies the Monge-Ampère equation but with the Dirichlet boundary condition,

$$u(x) = h(x), \ \forall x \in \partial \Omega.$$

The Dirichlet boundary condition is much easier than the second type boundary condition, hence Pogorelov problem can be solved more efficiently. Since the boundary  $\partial\Omega$  has zero measure, the Pogorelov map is also measure-preserving, and can replace the optimal transportation maps for many applications in practice for its efficiency and simplicity.

# 1.2 Discrete Alexandrov Maximum Principle

The work of [8] generalizes the Brenier theory to the discrete setting, which leads to a geometric variational algorithm to solve these problems. The algorithm optimizes a convex energy within a convex admissible solution space.

Fig. 1 shows an area-preserving parameterization example using this method.

The algorithm starts with an initial temporary solution. At each step, the algorithm finds a temporary solution  $u_k$  and the update direction  $d_k$  using Newton's method. Then we set an initial step length  $\lambda$  and update the temporary solution to  $u_{k+1} \leftarrow u_k + \lambda d_k$ . If  $u_{k+1}$  exceeds the admissible space, the algorithm cuts the step length to a half  $\lambda \leftarrow \lambda/2$ . We then adjust  $u_{k+1}$  accordingly, and verify again whether  $u_{k+1}$  is in the admissible space. This "damping process" is repeated until the updated temporary solution  $u_{k+1}$  is admissible. The damping procedure is the most time consuming step in the whole algorithm pipeline.

In the theory of Monge-Ampère equation, a priori estimate is an estimate for the size of a solution or its derivatives by the source and target measure, the geometry of the source and the target domain, without solving the PDE. If one has a priori estimate at the beginning, during the optimization the algorithm can utilize the estimate to restrict the range of the temporary solution, verify the admissibility of the temporary solution, hence improve the efficiency and robustness. The Alexandrov maximum principle is one of the most important priori estimate in the Monge-Ampère equation theory.

#### 1.3 Contributions

In this work, we focus on solving the Pogorelov problem and proving the discrete version of the Alexandrov maximum principle, which is further used to improve the computational efficiency of the proposed algorithm:

- 1. We develop a practical and efficient algorithm to solve the Pogorelov problem. The Pogorelov maps can be applied as a good approximation of the optimal transportation maps.
- 2. We generalize the classical Alexandrov maximum principle from the smooth setting to the discrete setting in theorem 3.5, and use it to improve the efficiency of the proposed algorithm.
- 3. We also conduct numerical experiments to test the efficiency of our algorithm when solving the Pogorelov problem, and verify the discrete version of the Alexandrov maximum principle.

The work is organized in the following way: in section 2, we briefly review the theory, computational algorithms and direct applications of optimal transportation maps; in section 3, we briefly recall the Brenier theorem in optimal transportation, the Alexandrov and Pogorelov theorems in convex geometry, and the geometric variational theorem. Then we prove the discrete Alexandrov maximum principle and formulate it as theorem 3.5; in section 4, we explain the details for solving the Pogorelov problem utilizing the Alexandrov maximum principle; the experimental results are reported in section 5. Finally the work is concluded in section 6.

### 2. RELATED WORK

This section briefly reviews the theory, algorithms and applications of optimal transportation. We refer readers to [9, 10] for a comprehensive review of the theory and [11] for computational algorithms.

#### 2.1 Theory

Monge raised the optimal transportation map problem as finding the most economical way to transfer

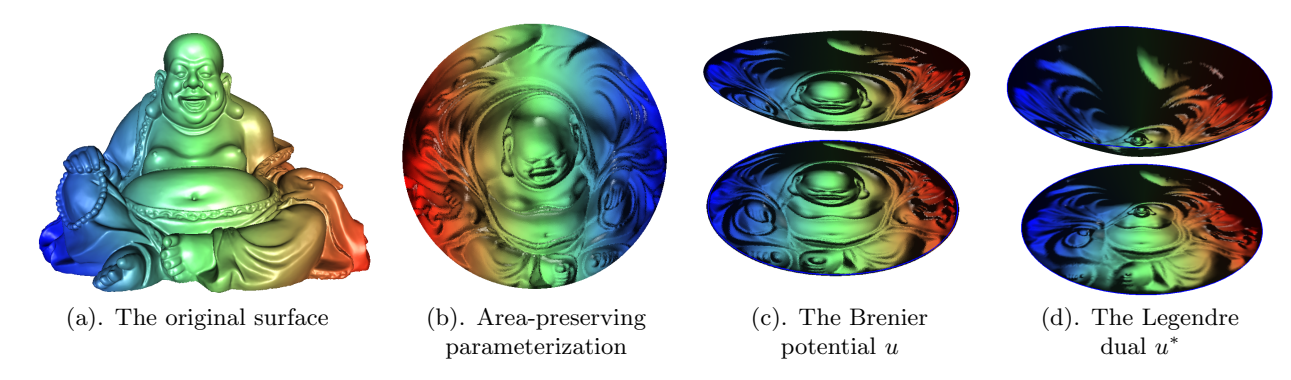


Figure 1: The area-preserving parameterization based on optimal transportation map. (a) shows the original Buddha surface  $(S,\mathbf{g})$ . The surface is conformally mapped onto the unit disk  $\varphi:(S,\mathbf{g})\to\mathbb{D}^2$ . The mapping pushes forward the surface area element to a measure  $\nu$  on  $\mathbb{D}^2$ . The optimal transportation map is calculated  $T:(\mathbb{D}^2,\mu)\to(\mathbb{D}^2,\nu)$ , where  $\mu$  is the uniform distribution. (c) shows the Brenier potential  $u:\mathbb{D}^2\to\mathbb{R}$ ,  $T=\nabla u$ . (d) shows the Legendre dual  $u^*(y)=\sup_{x\in\mathbb{D}^2}\{\langle x,y\rangle-u(x)\}$ .

one measure to the other in [12]. Kantorovich relaxed the transportation maps to transportation plans and solved the problem using linear programming [13, 14]. Brenier [7] discovered that the OT map is the gradient of a convex function, which satisfies the Monge-Ampère equation. Benamou-Brenier [15] developed the theory for solving OT maps using fluid dynamics. Comprehensive theories on optimal transportation can be found in [10, 16] and so on.

### 2.2 Algorithms

There are many methods for solving the optimal transportation problem, which can be classified into three main categories: Kantorovich approach, Brenier approach and Fluid dynamics approach.

The first approach is based on Kantorovich theorem, the optimal transportation problem is solved by using linear programming. De Goes [17] proposed the point-to-simplex algorithm which is similar to linear programming. Sinkhorn [18] method added an entropy regularizer to the Kantorovich prime problem and greatly improved the computational efficiency. The heat kernel was later used in [19, 20] to approximate the Wasserstein distance.

The second approach is based on the Brenier theorem, and the Brenier potential can be found by geometric optimization. Aurenhammer et al. [21] connected the OT map with power diagram in computational geometry. Then Gu et al. [8] connected the Brenier theory and the Alexandrov theory together, and proposed a geometric variational approach to solve the OT problem. De Goes et al. found the equivalence between capacity-constrained Voronoi tessellation and the OT problem in [22]. Levy [23] and Merigot et al. [24] proposed multi-scale approaches to accelerate the computation based on the Brenier theory for large-scale

optimal transportation problems. The computational optimal transportation methods through solving the Monge-Ampère equation have been generalized to the spherical cases by [5, 6, 25].

The third approach is based on Fluid dynamic theory. Benamou and Brenier developed a method [26] to solve the Monge-Ampère equation by minimizing the kinetic energy of flow field. Haker and Tananbaum [3] developed a method to compute the OT maps using fluid dynamics by removing the curl component from the vector field. However, it is still unclear whether Haker's method can obtain the optimal transportation map for high dimensional cases.

#### 2.3 Direct Applications

The optimal transportation has been used for the following applications: 2D shape reconstruction and simplification in [17], deformable 3D surface registration in [2], area-preserving surface parameterization [27], volume-preserving parameterization [28] and spherical texture mapping in [29]. The OT maps can also be applied for medical image registration [30], where the pixel intensity functions are treated as measure densities, area-preserving brain mappings [31], [32] and so on. Also, the OT maps can be used for virtual magnifier [1] and blue noise processing [22]. Furthermore, OT maps can be applied for reflector and refractor design [6, 33, 5], [34] and [35]. Optimal transportation also plays an essential role in deep learning field related to generative models [36, 37, 38, 39, 40, 41].

In most of the above applications, the optimal transportation maps can be replaced by other measure-preserving maps. The Pogorelov map is a good candidate due to its computational simplicity and efficiency. Currently, most existing algorithms aim at solving the optimal transportation problem, or equivalently the

Alexandrov problem, and few of them choose to tackle the Pogorelov problem. In contrast, our work in this paper focuses on solving the Pogorelov problem. Furthermore, we haven't found any existing works that utilize the Alexandrov maximum principle in the geometric modeling and processing fields, which is another focus of the current work.

### 3. THEORETICAL FOUNDATION

In this section, we briefly review the theoretical foundation of optimal transportation and convex geometry, including the Brenier theorem, the Alexandrov theorem, and the Pogorelov theorem. We then prove the discrete version of the Alexandrov maximum principle.

### 3.1 Optimal Transportation

Suppose  $\Omega, \Omega^* \subset \mathbb{R}^d$  are domains in an Euclidean space, with probability measures  $\mu$  and  $\nu$  respectively satisfying the equal total mass condition:  $\mu(\Omega) = \nu(\Omega^*)$ . The density functions are  $d\mu = f(x)dx$  and  $d\nu = g(y)dy$ . The transportation map  $T: \Omega \to \Omega^*$  is measure preserving, if for any Borel set  $B \subset \Omega^*$ ,

$$\int_{T^{-1}(B)} d\mu(x) = \int_B d\nu(y),$$

denoted as  $T_{\#}\mu = \nu$ . Monge raised the *optimal transportation problem*: given the *transportation cost function*  $c: \Omega \times \Omega^* \to \mathbb{R}^+$ , find a measure preserving map  $T: \Omega \to \Omega^*$  that minimizes the *total transportation cost*.

$$(MP) \quad \min\left\{ \int_{\Omega} c(x, T(x)) d\mu(x) : T_{\#}\mu = \nu \right\}.$$

The above equation gives the Monge problem (MP) and the minimizer is called the *optimal transportation* map (OT map). The transportation cost of the OT map is called the *OT cost* between the measures.

**Theorem 3.1** (Gu et al. [7]). Suppose the measures  $\mu$  and  $\nu$  are with compact supports  $\Omega, \Omega^* \subset \mathbb{R}^d$  respectively, and they have equal total mass  $\mu(\Omega) = \nu(\Omega^*)$ . Assume the corresponding density functions are given by  $f, g \in L^1(\mathbb{R}^d)$ , and the cost function is  $c(x, y) = \frac{1}{2}|x-y|^2$ , then the optimal transportation map from  $\mu$  to  $\nu$  exists and is unique. It is the gradient of a convex function  $u: \Omega \to \mathbb{R}$ , the so-called Brenier potential, u is unique up to adding a constant, and the OT map is given by  $T = \nabla u$ .

If the Brenier potential is  $\mathbb{C}^2$ , then by measure preserving condition, it satisfies the Monge-Ampère equation,

$$\det D^2 u(x) = \frac{f(x)}{g \circ \nabla u(x)}, \quad s.t. \nabla(\Omega) = \Omega^*, \qquad (1)$$

where  $D^2u$  is the Hessian matrix of u and the unique OT map is given by  $T = \nabla u$ .

#### 3.2 Geometric Variational Method

If u is not smooth, we can still define the Alexandrov solution. The sub-gradient of a convex function u at x is defined as

$$\partial u(x) := \left\{ p \in \mathbb{R}^d : u(z) \ge \langle p, z - x \rangle + u(x), \forall z \in \Omega \right\}$$

The sub-gradient defines a set-valued map:  $\partial u: \Omega \to \Omega^*$ ,  $x \mapsto \partial u(x)$ . We can use the sub-gradient map to replace the gradient map in the Monge-Ampère equation Eqn. (1), and define the Alexandrov Solution as follows:

**Definition 3.1** (Alexandrov Solution [42]). If a convex function  $u: \Omega \to \mathbb{R}$  satisfies the equation  $(\partial u)_{\#}\mu = \nu$ , or equivalently  $\mu((\partial u)^{-1}(B)) = \nu(B)$ , for all Borel set  $B \subset \Omega^*$ , then u is called an Alexandrov solution to the Monge-Ampère equation Eqn. (1).

The Alexandrov problem aims at finding a convex polyhedron with prescribed face normals and face areas. In smooth case, the Alexandrove problem finds the convex surface with prescribed Gaussian curvature. Both the Alexandrove problem and the Brenier problem are governed by the same Monge-Ampère equation. Therefore, solving the Alexandrov problem is equivalent to computing the Brenier potential, which is given by the Alexandrov Solution. The work of [8] proves a geometric variational approach for computing the Alexandrov solution of the semi-discrete optimal transportation problem.

# 3.3 Semi-discrete Optimal Transportation

As shown in Fig. 2, suppose the source measure is  $(\Omega, \mu)$ ,  $\Omega$  is a compact convex domain with non-empty interior in  $\mathbb{R}^d$ , the density function f(x) is continuous. In practice, the target measure  $(\Omega^*, \nu)$  is usually discretized as  $\nu = \sum_{i=1}^n \nu_i \delta(y - p_i)$ , where  $p_1, \ldots, p_n \subset \mathbb{R}^d$  are distinct n points and  $\nu_1, \ldots, \nu_n > 0$  so that  $\sum_{i=1}^n \nu_i = \mu(\Omega)$ . In this situation, the discrete Brenier potential is a piecewise linear convex function. In fact, there exists a height vector  $\mathbf{h} = (h_1, \ldots, h_n) \in \mathbb{R}^n$ , so that the upper envelope  $u_{\mathbf{h}}$  of the hyper-planes  $\pi_i(x) := \langle x, p_i \rangle + h_i$  defined as

$$u_{\mathbf{h}}(x) = \max_{i=1}^{n} \{ \langle x, p_i \rangle + h_i \}, \tag{2}$$

gives the discrete Brenier potential, as shown in the top frame of Fig. 2(c). The projection of the envelope  $\operatorname{Env}(\{\pi_i\}_{i=1}^n)$  induces a power diagram (the bottom frame of Fig. 2(c)),

$$\mathbb{R}^d = \bigcup_{i=1}^n W_i(\mathbf{h}), \quad W_i(\mathbf{h}) := \{ x \in \mathbb{R}^d : \nabla u_{\mathbf{h}} = p_i \}.$$

The  $\mu$ -volume of each cell  $\mu(W_i(\mathbf{h}) \cap \Omega) = \nu_i$ , the semi-discrete optimal transportation map is given by  $\nabla u_{\mathbf{h}}$ ,

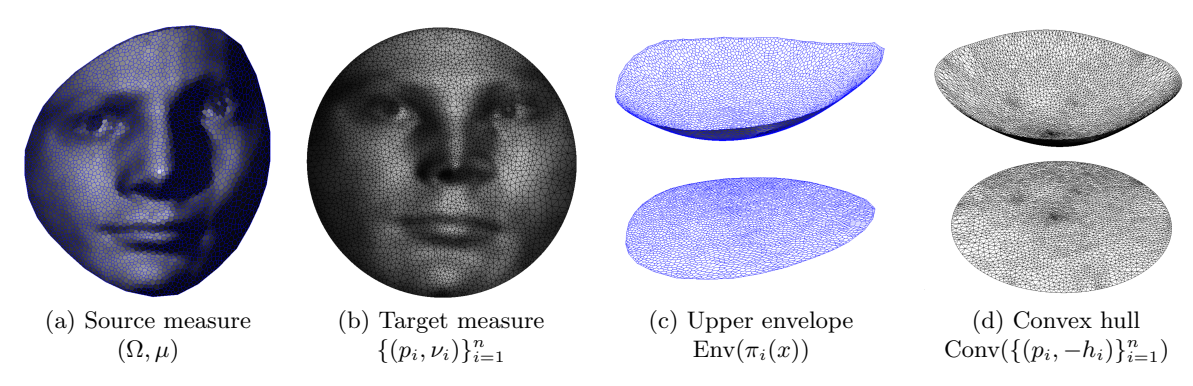


Figure 2: (a) The continuous source domain  $\Omega$  is with uniform distribution  $\mu$ . (b) The discrete target measure is  $\nu:=\sum_{i=1}^n\nu_i\delta(y-p_i)$  with  $p_i$ s the vertices. (c) The Brenier potential  $u:\Omega\to\mathbb{R}$  is the upper envelope of the planes  $\pi_i(x)=\langle p_i,x\rangle+h_i$ , as shown in the top frame. The cell decomposition induced by the Brenier potential gives the OT map, each cell  $W_i$  in  $\Omega$  (shown in the bottom frame) is mapped to the corresponding  $p_i$  with  $\mu(W_i)=\nu_i$ . (d) The Legendre dual  $u^*$  of the Brenier potential u is the convex hull of points  $\{(p_i,-h_i)\}_{i=1}^n$ . Please zoom in/out for better visualization.

or equivalently  $W_i(\mathbf{h}) \cap \Omega \mapsto p_i$ . The discrete Brenier potential can be obtained by optimizing the following convex energy:

**Theorem 3.2** (Gu et al. [8]: Alexandrov). Let  $\Omega$  be a compact convex domain in  $\mathbb{R}^d$ ,  $\{p_1, ..., p_n\}$  be a set of distinct points in  $\mathbb{R}^d$  and  $f: \Omega \to \mathbb{R}$  be a positive continuous function. Then for any  $\nu_1, ..., \nu_n > 0$  with  $\sum_{i=1}^n \nu_i = \int_{\Omega} f(x) dx$ , there exists  $\mathbf{h} = (h_1, h_2, ..., h_n) \in \mathbb{R}^n$ , unique up to adding a constant (c, c, ..., c), so that

$$\mu(W_i(\mathbf{h})\cap\Omega) = \int_{W_i(\mathbf{h})\cap\Omega} f(x)dx = \nu_i \quad \forall i = 1, 2, \dots, n.$$
(3)

The height vector  $\mathbf{h}$  is exactly the minimal solver of the convex function

$$E(\mathbf{h}) = \int_0^{\mathbf{h}} \sum_{i=1}^n \mu(W_i(\mathbf{h}) \cap \Omega) dh_i - \sum_{i=1}^n h_i \nu_i$$
 (4)

on the open convex set (the admissible solution space)

$$\mathcal{H} = \{ \mathbf{h} \in \mathbb{R}^n | \mu(W_i(\mathbf{h}) \cap \Omega) > 0, \ i \in \{1, 2, \dots, n\} \}$$
$$\cap \left\{ \sum_{i=1}^n h_i = 0 \right\}$$
(5)

Furthermore, the gradient map  $\nabla u_{\mathbf{h}}$  minimizes the quadratic cost  $\frac{1}{2} \int_{\Omega} |x - T(x)|^2 f(x) dx$  among all the measure preserving transportation maps  $T: (\Omega, \mu) \to (\mathbb{R}^d, \nu = \sum_{i=1}^n \nu_i \delta(y - p_i)), T_{\#}\mu = \nu$ .

According to [43],  $E(\mathbf{h})$  is continuous and a  $C^2$  function on the admissible space, since its Hessian matrix is continuous.

### 3.4 Convex Geometry

The Brenier potential in the optimal transportation theory can be reformulated as the classical Alexandrov problem and the Pogorelov problem, both of them satisfying the Monge-Ampére equation. In the discrete version, the Alexandrov problem aims at finding a convex polyhedron with user prescribed face normals and areas.

**Theorem 3.3** (Alexandrov 1950). Given a compact convex domain  $\Omega \subset \mathbb{R}^d$ , and  $p_1, \dots, p_n$  are distinct points in  $\mathbb{R}^d$ ,  $\nu_1, \nu_2, \dots, \nu_n > 0$ , such that  $\sum \nu_i = Vol(\Omega)$ , there exists a piecewise linear (PL) convex function

$$u(x) := \max\{\langle x, p_i \rangle + h_i, i \in \{1, 2, \dots, n\}\}$$

unique up to translation such that

$$Vol(W_i) = Vol(\{x | \nabla u(x) = p_i\}) = \nu_i.$$

The graph of u(x) is called the Alexandrov polyhedron, which is an open convex polyhedron with infinite boundary faces. Alexandrov's proof is topological, not variational. In fact, the Alexandrov potential is exactly the discrete Brenier potential. Hence, theorem 3.2 also gives the solution to the Alexandrov problem.

The Pogorelov problem is very similar to the Alexandrov problem, and it is equivalent to solving the Monge-Ampère equation with the Dirichlet boundary condition:

$${\rm det} D^2 u(x) = \frac{f(x)}{g \circ \nabla u(x)}, \quad s.t. \ \ u(x) = h(x) \ \forall x \in \partial \Omega.$$

Basically, the supporting planes of the infinite boundary faces of the Alexandrov polyhedron are fixed and the slopes of the other supporting planes are fixed, but their heights can be changed. Given any desired positive  $\nu_i$ s, there exists a set of unique heights  $h_i$ s, such that the area of the *i*-th face equals to  $\nu_i$ . Gu et al. [8] also proved a variational approach to solve the Pogorelov problem:

Theorem 3.4 (Gu et al. [8]: Pogorelov).  $Conv(v_1,\cdots,v_m)$  $Suppose \Omega =$ is a ddimensional compact convex polytope in  $\mathbb{R}^d$ that  $v_i \notin Conv(v_1, \ldots, v_{i-1}, v_{i+1}, \ldots, v_m)$  for all  $i \in \{1, 2, ..., m\}$  and  $p_1, ..., p_n$  are in the interior of  $\Omega$ . For any  $g_1, \ldots, g_m \in \mathbb{R}$  and  $\nu_1, \nu_2, \ldots, \nu_n > 0$ , there exists a convex cell decomposition T having  $v_i$  and  $p_j$  as vertices and a piecewise linear convex function  $u:(\Omega,T)\to\mathbb{R}$  so that  $u(v_i)=g_i$ ,  $i \in \{1, 2, ..., m\}$  and the Lebesgue measure of the sub-gradient of u at  $p_i$  is  $\nu_i$ ,  $j \in \{1, 2, ..., n\}$ . In fact, the solution u is the Legendre dual of

$$\max\{\langle x, p_j \rangle + h_j, \langle x, v_i \rangle - g_i | i \in \{1, 2, \dots, m\}; j \in \{1, 2, \dots, n\}\}$$

and  $\mathbf{h} = (h_1, h_2, \dots, h_n)$  is the unique critical point of a strictly convex function,

$$E(\mathbf{h}) = \int_0^{\mathbf{h}} \sum_{j=1}^n \mu(W_j(\mathbf{h})) dh_j - \sum_{j=1}^n h_j \nu_j, \quad (6)$$

on the open set (admissible solution space)

$$\mathcal{H} = \{ \mathbf{h} \in \mathbb{R}^n | W_j(\mathbf{h}) \neq \emptyset, \forall j \in \{1, 2, \dots, n\} \}.$$
 (7)

The detailed difference between the solutions of the Alexandrov problem and the Pogorelov problem can be found in Fig. 3.

# 3.5 Discrete Alexandrov Maximum Principle

**Definition 3.2** (Convex Piecewise Linear Function). Let  $P = \{p_1, p_2, \ldots, p_n\} \subset \mathbb{R}^d$  be a set of distinct points,  $\Omega := \operatorname{Conv}(\{p_1, p_2, \ldots, p_n\})$  be the convex hull of P. Given a discrete function  $u: P \to \mathbb{R}$ ,  $u(p_i)$  is denoted as  $u_i$ , it can be extended to a convex piecewise linear function  $\hat{u}: \Omega \to \mathbb{R}$ . The graph of  $\hat{u}$  is the convex hull of points  $\{(p_1, u_1), (p_2, u_2), \ldots, (p_n, u_n)\}$ .

Note that the triangulations of different piecewise linear functions are different. Given two discrete functions  $u, v : P \to \mathbb{R}$ , if  $u_i < v_i$ ,  $\forall p_i \in P$ , then  $\hat{u}(x) < \hat{v}(x)$ ,  $\forall x \in \text{Conv}(P)$ .

**Lemma 3.1** (Monotonicity of sub-gradient). Let  $P = \{p_1, p_2, \ldots, p_n\} \subset \mathbb{R}^d$  be a set of distinct points,  $\Omega := Conv(\{p_1, p_2, \ldots, p_n\})$  be the convex hull of P. Let  $\{p_{i_1}, p_{i_2}, \cdots, p_{i_l}\} \subset P$ ,  $O = Conv(\{p_{i_1}, p_{i_2}, \cdots, p_{i_l}\})$  be an open bounded set, and  $u, v : P \to \mathbb{R}$  be two discrete functions defined on P, and their extentions,

the convex piecewise-linear functions  $\hat{u}, \hat{v}: \Omega \to \mathbb{R}$ , satisfying:

$$\left\{ \begin{array}{lll} \hat{u} = \hat{v} & on & \partial O \\ \hat{u} \leq \hat{v} & in & O \end{array} \right.$$

Then the images of the sub-gradient maps satisfy

$$\partial \hat{v}(O) \subset \partial \hat{u}(O),$$

and in particular,  $\mu_{\hat{u}}(O) \ge \mu_{\hat{v}}(O)$ , where

$$\mu_{\hat{u}}(E) := \big|\bigcup_{x \in E} \partial \hat{u}(x)\big|.$$

| · | representing the Lebesque measure.

*Proof.* Let  $p \in \partial \hat{v}(x)$  for some  $x \in O$ , then the affine function  $l_{x,p}(z) := \hat{v}(x) + \langle p, z - x \rangle$  touches  $\hat{v}$  from below at x. Since  $\hat{u} \leq \hat{v}$ , the constant

$$a := \max_{z \in \bar{O}} l_{x,p}(z) - u(z)$$

is non-negative and that  $l_{x,p} - a$  touches  $\hat{u}$  from below at some point  $x_0 \in \bar{O}$ . There are two cases here:

case 1.  $x_0 \in O$ , then  $w := \hat{u} - (l_{x,p} - a)$  attains a local minimum at  $x_0$ , which is also a global minimum by the convexity of w, namely

$$l_{x,p} - a \le u \text{ in } \Omega \quad l_{x,p}(x_0) - a = u(x_0),$$

and  $p \in \partial \hat{u}(x_0) \subset \partial \hat{u}(O)$ , as desired. case 2:  $x_0 \in \partial O$ . Since  $\hat{u} = \hat{v}$  on  $\partial O$  and  $x_0 \in \partial O$ , we obtain that a = 0. Therefore,

$$l_{x,p} \leq u \leq v$$
 in  $O$ .

As  $l_{x,p}(x) = \hat{v}(x)$ , this gives  $l_{x,p}(x) = \hat{u}(x)$ . So  $l_{x,p}$  touches  $\hat{u}$  from below at x and  $p \in \partial u(x)$ , which concludes the proof.

A consequence of the monotonicity result is the discrete Alexandrov maximum principle.

**Theorem 3.5** (Discrete Alexandrov Maximum Principle). Let  $P = \{p_1, p_2, \ldots, p_n\} \subset \mathbb{R}^d$  be a set of distinct points,  $\Omega := Conv(\{p_1, p_2, \ldots, p_n\})$  be the convex hull of P, and let  $u : \Omega \to \mathbb{R}$  be a piecewise-linear convex function such that u = 0 on  $\partial \Omega$ . Then there exists a dimensional constant  $C_d > 0$  such that

$$|u(x)|^d \le C_d \operatorname{diam}(\Omega)^{d-1} \operatorname{dist}(x, \partial \Omega) |\partial u(\Omega)| \quad \forall x \in \Omega.$$
(8)

*Proof.* Let  $p_i \in P$ ,  $(p_i, u_i)$  be a point on the graph of u, and consider the convex cone function  $y \mapsto C_{p_i}(y)$ , with vertex at  $(p_i, u_i)$  that vanishes on  $\partial\Omega$ . By the convexity of u, we have  $u \leq C_{p_i}$  in  $\Omega$ . The monotonicity of subdifferential 3.1 implies

$$|\partial C_{p_i}(p_i)| \le |\partial C_{p_i}(\Omega)| \le |\partial u(\Omega)|;$$
 (9)

In the following, we bound  $|\partial C_{p_i}(p_i)|$  from below.

Step 1.  $\partial C_{p_i}(p_i)$  contains the ball  $B_{\rho}(0)$  with  $\rho := |u_i|/\text{diam}(\Omega)$ . Take q with  $|q| < |u_i|/\text{diam}(\Omega)$ , and consider the affine function

$$l_{p_i,q}(z) := u_i + \langle q, z - p_i \rangle.$$

Then we have  $l_{p_i,q}(p_i) = u_i = C_{p_i}(p_i)$  and

$$l_{p_i,q}(z) \le u_i + |q||z - p_i| \le u_i + |q| \operatorname{diam}(\Omega) \le 0 \quad \forall z \in \partial \Omega,$$

By convexity  $l_{p_i,q} \leq C_{p_i}$  inside  $\Omega$ . Hence,  $l_{p_i,q}$  touches  $C_{p_i}$  from below at  $p_i$ , which implies that  $q \in \partial C_{p_i}(p_i)$ . By the arbitrariness of q, this proves that  $\partial C_{p_i}(p_i) \supset B_{\rho}(0)$ , as desired.

Step 2.  $\partial C_{p_i}(p_i)$  contains a vector of norm  $|u_i|/\mathrm{dist}(x,\partial\Omega)$ . Consider a point  $p_j \in \partial\Omega$ , such that  $|p_i - p_j| = \mathrm{dist}(p_i,\partial\Omega)$ , and set

$$q := \frac{p_j - p_i}{|p_j - p_i|} \frac{|u_i|}{\operatorname{dist}(p_i, \partial\Omega)}.$$

Then  $l_{p_i,q}(z) := u_i + \langle q, p_i - z \rangle$  satisfies

$$l_{p_i,q}(p_i) = u_i + \langle q, p_i - p_i \rangle = u_i + |u_i| = 0,$$

and the hyperplane  $\{l_{p_i,q}=0\}$  is tangent to  $\Omega$  at  $p_j$ . This implies that  $l_{p_i,q}\leq 0=C_{p_i}$  on  $\partial\Omega$ . In fact, given any  $z\in\partial\Omega$ , we have that  $\mathrm{dist}(p_i,\partial\Omega)\leq |z-p_i|$ , so

$$l_{p_i,q}(z) \le u_i \left(1 - \frac{z - p_i}{\operatorname{dist}(p_i, \partial\Omega)}\right) \le 0.$$

Arguing as in Step 1, this shows that  $q \in \partial C_{p_i}(p_i)$ .

Step 3. By Step 1 and Step 2, we know that

$$\partial C_{p_i}(p_i) \supset B_{\varrho}(0) \cup \{q\},$$
 (10)

where  $\rho = |u_i|/\text{diam}(\Omega)$  and  $|q| = |u_i|/\text{dis}(p_i, \partial \Omega)$ . Let  $\Sigma_{\rho}$  denote the intersection of  $B_{\rho}(0)$  with the hyperplane passing through the origin and orthogonal to q,

$$\Sigma_{\rho} := B_{\rho}(0) \cap \{z : \langle z, q \rangle = 0\}.$$

Since  $\partial C_{p_i}(p_i)$  is convex, by Eqn.(10) it contains the cone  $\mathcal{C}$  generated by q and  $\Sigma_{\rho}$ . Hence

$$|\partial C_{p_i}(p_i)| \ge |\mathcal{C}| = C_d |q| \rho^{d-1} = C_d \frac{|u_i|^d}{\operatorname{diam}(\Omega)^{d-1} \operatorname{dist}(p_i, \partial \Omega)},$$

where  $C_d > 0$  is the dimensional constant,  $C_2 = 1$  and

$$C_d = \frac{1}{d} \frac{\pi^{\frac{d-1}{2}}}{\Gamma(\frac{d-1}{2} + 1)}$$

Now, assume x is an arbitrary point in  $\Omega$ , we can repeat the same argument and the inequality (8) still holds. This concludes the proof.

### 4. COMPUTATIONAL ALGORITHMS

This section explains the algorithmic details to solve the Monge-Ampère equation with with the Dirichlet boundary condition, namely the Pogorelov problem. The algorithm is implemented using computational geometric method, hence we start with the fundamental concepts in computational geometry [44].

# 4.1 Basic Concepts from Computational Geometry

A hyperplane in  $\mathbb{R}^{d+1}$  is represented as  $\pi(x) := \langle p, x \rangle + h$ ,  $x \in \mathbb{R}^d$ ,  $h \in \mathbb{R}$ . Given a family of hyperplanes  $\{\pi_i(x) = \langle p_i, x \rangle + h_i\}_{i=1}^n$ , their *upper envelope* denoted as  $\operatorname{Env}(\{\pi_i\}_{i=1}^n)$  is the graph of the function

$$u(x) := \max_{i=1}^{n} \left\{ \langle p_i, x \rangle + h_i \right\}.$$

The Legendre dual of u is defined as

$$u^*(y) := \max_{x \in \mathbb{R}^d} \{ \langle x, y \rangle - u(x) \}.$$

Each hyperplane  $\pi_i(x)$  has a dual point in  $\mathbb{R}^{d+1}$ ,  $\pi_i^* := (p_i, -h_i)$ , and the graph of  $u^*$  is the lower convex hull of the dual points  $\{\pi_i^*\}_{i=1}^n$ , which is the minimal convex set containing  $\{\pi_i^*\}_{i=1}^n$ . The projection of the upper envelope induces a nearest power diagram  $\mathcal{D}(\Omega)$  of  $\Omega$ .

$$\Omega = \bigcup_{i=1}^{n} W_i(u), \ W_i(u) := \{x \in \Omega | \nabla u(x) = p_i \}.$$

The projection of the lower convex hull  $u^*$  induces a nearest weighted Delaunay triangulation  $\mathcal{T}(\Omega^*)$  of  $\Omega^*$ .  $\mathcal{D}(\Omega)$  and  $\mathcal{T}(\Omega^*)$  are dual to each other, namely  $p_i$  connects  $p_j$  in  $\mathcal{T}(\Omega^*)$  if and only if  $W_i(u)$  is adjacent to  $W_j(u)$ . Fig. 1 and Fig. 2 show these basic concepts.

#### 4.2 Algorithm Pipeline

The algorithm mainly optimizes the energy  $E(\mathbf{h})$  of Eqn. (6) in the admissible solution space  $\mathcal{H}$  in Eqn. (7) using Newton's method. Assume the interior vertices are  $\{p_i\}_{i=1}^n$  and the boundary vertices are  $\{q_i\}_{i=1}^m$ . At the beginning, the height vector  $\mathbf{h}_0$  is initialized as  $h_i = \frac{1}{2}(|p_i|^2 - 1)$  for each interior vertex  $p_i$ , and as the fixed constant  $g_i$  for each boundary vertex  $g_i$  respectively. At each step, the convex hull of  $\{(p_i, -h_i)\}_{i=1}^n \cup$  $\{(q_j, +g_j)\}_{j=1}^m$  is constructed. The lower convex hull is projected to induce a nearest weighted Delaunay triangulation  $\mathcal{T}$  of  $\{p_i\} \cup \{v_i\}$ . Each interior vertex on the convex hull  $v_i(\mathbf{h}) = (p_i, -h_i)$  corresponds to a supporting plane  $\pi_i(\mathbf{h}, x) = \langle p_i, x \rangle + h_i$ , each boundary vertex  $v_i = (q_i, g_i)$  corresponds to a supporting plane  $\pi_i(\mathbf{h}, x) = \langle q_j, x \rangle - g_j$ . Each face  $[v_i, v_j, v_k]$  in the convex hull is dual to the vertex in the envelope, which is the intersection point of  $\pi_i, \pi_j$  and  $\pi_k$ . The lower convex hull is dual to the upper (lower) envelope. The projection of the upper envelope induces the nearest power diagram. The relationship is given in Fig. 2(c) and Fig. 2(d).

```
Algorithm 1: Solving Pogorelov Problem
Input: \Omega = \text{Conv}(q_1, q_2, \dots, q_m), boundary
            (g_1, g_2, \ldots, g_m), \{(p_i, \nu_i)\}_{i=1}^n \subset \Omega \times R
Output: The height vector h of the Pogorelov
               Polyhedron u_{\mathbf{h}}
Initialize u(q_j) = g_j, h_i = \frac{1}{2}(|p_i|^2 - 1);
while true do
     Compute the lower convex hull of
       \{(p_i, -h_i)\}_{i=1}^n \cup \{(q_j, +g_j)\}_{j=1}^m;
     Compute the upper envelope of the planes
       \{\langle p_i, x \rangle + h_i\}_{i=1}^n \cup \{\langle q_j, x \rangle - g_j\}_{j=1}^m;
     Project the upper envelope to the plane to get
       a nearest power diagram
       \Omega = \bigcup_{i=1}^n W_i(\mathbf{h}) \bigcup_{j=1}^m U_j(\mathbf{h}), \text{ where } W_i(\mathbf{h})'s
      are finite, U_i(\mathbf{h})'s are infinite cells;
     Compute the \mu-volume of each finite cell
       w_i(\mathbf{h}) = \mu(W_i(\mathbf{h})) using Eqn. (11);
     Compute the gradient of the energy E(\mathbf{h})
       using Eqn. (12), \nabla E(\mathbf{h}) = (\nu_i - w_i(\mathbf{h}));
     if \|\nabla E(\mathbf{h})\| < \varepsilon then
         return h;
     end
     Compute the \mu-lengths of the power Voronoi
      edges W_i(\mathbf{h}) \cap W_i(\mathbf{h});
     Construct the Hessian matrix of the energy
       \operatorname{Hess}(E(\mathbf{h})) := \frac{\partial^2 E(\mathbf{h})}{\partial h_i \partial h_j} = \frac{\mu(W_i(\mathbf{h}) \cap W_j(\mathbf{h}))}{|p_i - p_j|}
       Solve the linear system:
      \operatorname{Hess}(E(\mathbf{h}))\mathbf{d} = \nabla E(\mathbf{h});
     \lambda \leftarrow 1;
     repeat
          if h + \lambda d violates the Alexandrov
            maximum principle then
               \lambda \leftarrow \frac{1}{2}\lambda;
               continue;
          end
          Compute the nearest power diagram
            \mathcal{D}(\mathbf{h} + \lambda \mathbf{d});
     until no empty power cell;
     Update the height vector \mathbf{h} \leftarrow \mathbf{h} + \lambda \mathbf{d};
end
```

Then we compute the  $\mu$ -volume of each power cell using

$$w_i(\mathbf{h}) := \int_{W_i(\mathbf{h})} f(x) dx, \tag{11}$$

and the gradient of the energy Eqn. (6) is given by

$$\nabla E(\mathbf{h}) = (\nu_1 - w_1(\mathbf{h}), \nu_2 - w_2(\mathbf{h}), \dots, \nu_n - w_n(\mathbf{h})).$$
(12)

The Hessian matrix  $\operatorname{Hess}(E(\mathbf{h}))$  can be constructed as follows: for off diagonal elements,

$$\frac{\partial^2 E(\mathbf{h})}{\partial h_i \partial h_j} = \frac{\partial w_i(\mathbf{h})}{\partial h_j} = \frac{-1}{|p_i - p_j|} \int_{W_i(\mathbf{h}) \cap W_j(\mathbf{h})} f(x) dx = -\frac{\mu(\bar{e}_{ij})}{|e_{ij}|}.$$
(13)

where  $e_{ij}$  is the edge in the weighted Delaunay triangulation  $\mathcal{T}(\mathbf{h})$  connecting  $p_i$  and  $p_j$ ,  $\bar{e}_{ij}$  is the dual edge in the power diagram  $\mathcal{D}(\mathbf{h})$ ; and for diagonal elements,

$$\frac{\partial^2 E(\mathbf{h})}{\partial h_i^2} = \frac{\partial w_i(\mathbf{h})}{\partial h_i} = \sum_{j \in N(i)} \frac{\mu(\bar{e}_{ij})}{|e_{ij}|}.$$
 (14)

where N(i) is the set of the neighbours of the *i*th vertex. Then we solve the following linear system to find the update direction,

$$\operatorname{Hess}(E(\mathbf{h}))\mathbf{d} = \nabla E(\mathbf{h}). \tag{15}$$

Finally we need to determine the step length  $\lambda$ , such that  $\mathbf{h} + \lambda \mathbf{d}$  is still in the admissible solution space  $\mathcal{H}$ ,

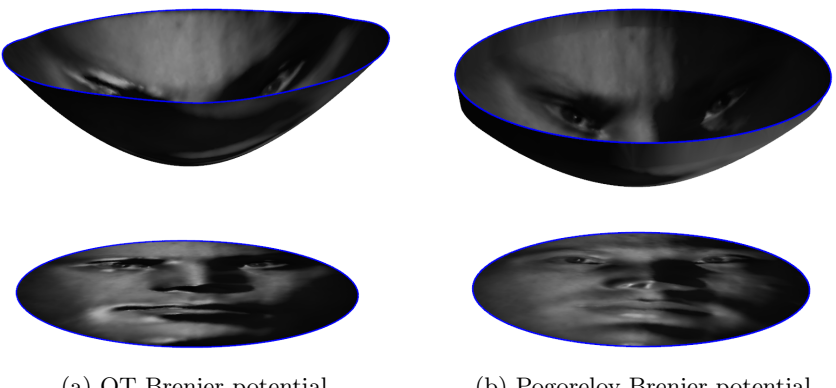
$$\mathcal{H} = \{ \mathbf{h} \in \mathbb{R}^n | \mu(W_i(\mathbf{h})) > 0, \ i = 1, 2, \dots, n \}.$$
 (16)

We initially set the step length  $\lambda$  to be -1, if  $\mathbf{h} + \lambda \mathbf{d}$ violates the Alexandrov maximum principle, then we cut  $\lambda$  to a half,  $\lambda \leftarrow 1/2\lambda$ , and iterate again. Then we further compute the power diagram  $\mathcal{D}(\mathbf{h}+\lambda\mathbf{d})$ . If some cells disappear in the power diagram, meaning  $\mathbf{h} + \lambda \mathbf{d}$ exceeds the admissible space, then we cut  $\lambda$  by half and iterate again. We repeat this process, until we find an appropriate step length  $\lambda$  so that  $\mathbf{h} + \lambda \mathbf{d}$  is in the admissible space (Eqn. (7)) and satisfies the discrete Alexandrov maximum principle Thm. 3.5. Then we update **h** as  $\mathbf{h} + \lambda \mathbf{d}$ . We repeat the above procedures until the norm of the gradient of the energy is less than a prescribed threshold  $\varepsilon$ . Each nearest power cell  $W_i(\mathbf{h})$  corresponding to the sample point  $p_i$  will be of the desired measure  $\nu_i$ . We conclude our algorithm for solving the Pogorelov problem in Alg. 1.

During the optimization, the connectivity of the power diagram keeps changing. Instead of constructing the convex hull from scratch at every step, we can locally modify the connectivity through a variation of Lawson's edge flip algorithm [45] to improve the efficiency. Furthermore, in order to improve the numerical stability, we can use adaptive arithmetic during the construction of convex hulls.

#### 5. EXPERIMENTS

We conduct experiments to test the efficacy and efficiency of the proposed Pogorelov map algorithm, and verify the discrete Alexandrov maximum principle.



(a) OT Brenier potential (b) Pogorelov Brenier potential

Figure 3: The potentials of the OT problem and the Pogorelov problem. The blue curves give the boundary of the potentials.

### 5.1 Experimental setup

All the algorithms are developed using generic C++ compatible with Windows and Linux platforms. We mainly use Eigen [46] for the numerical computations and OpenGL for the user interface. The surface meshes are represented by the half-edge data structure. All the experiments are conducted on a Windows laptop with Intel Core i7-7700HQ CPU and 16 GB memory.

#### 5.2 Source and Target Measures

In order to test the proposed Pogorelov map algorithm Alg. 1 and verify that the solution does satisfy the Alexandrov maximum principle, we conduct several experiments. The source measure  $d\mu = f dx$  is the uniform distribution defined on the planar unit disk  $\Omega = \mathbb{D}^2$ . We set three target measures  $(\Omega^*, \nu)$ .

Case 1. As shown in Fig. 5, the male facial surface  $(S, \mathbf{g})$  in frame (a) is represented as a triangle mesh with 14,358 vertices and 28,328 faces. The surface is conformally mapped to the unit disk via discrete surface Ricci flow [47], the mapping is denoted as  $\varphi: S \to \mathbb{D}^2$ . The conformal mapping image is shown in frame (b). The images of the boundary vertices are  $q_j = \varphi(v_j), \ v_j \in \partial S, \ j \in \{1,2,\ldots,m\}$ . The convex hull of  $q_j$ 's is  $\mathrm{Conv}(\{q_j\}_{j=1}^m)$ . The images of the interior vertices are  $p_i = \varphi(v_i), \ v_i \notin \partial S, \ i \in \{1,2,\ldots,n\}$ . The images of the interior vertices, fall inside the convex hull of the images of the boundary vertices, namely  $\{p_i\}_{i=1}^n \subset \mathrm{Conv}(\{q_j\}_{j=1}^m)$ . The target domain  $\Omega^*$  is the union of the images of interior vertices,

$$\Omega^* := \{p_1, p_2, \dots, p_n\}.$$

The discrete measure  $\nu_i$  corresponding to an interior vertex  $v_i$  is the area of the neighborhood of  $v_i$  on the

surface, computed as

$$\nu_i = \frac{1}{3} \sum_{[v_i, v_j, v_k] \in S} area([v_i, v_j, v_k])$$
 (17)

where  $[v_i, v_j, v_k]$  represents a face adjacent to  $v_i$  on the original mesh in  $\mathbb{R}^3$ . The target measure is the summation of Dirac measures  $\nu = \sum_{i=1}^n \nu_i \delta(y-p_i)$ . The measure for the boundary vertices is irrelevant. For the purpose of visualization, the summation of the discrete measures is normalized to the area of  $\Omega$ , namely  $\pi$ . In this case, the solution to the Pogorelov problem gives us an area-preserving map of the facial surface.

Case 2. The discrete measure  $\nu_i$  for each interior vertex  $v_i$  is set to be 1/n, where n is the number of the interior vertices, namely target measure  $\nu$  is the uniform distribution on  $\Omega^*$ .

Case 3. The discrete measures for the interior vertices are randomly sampled from the uniform distribution. Then we normalize the target measure so that the summation of the discrete measures is equal to the area of the source domain.

# 5.3 Discrete Alexandrov Maximum Principle

For the Pogorelov map, we initialize the heights to be 0 for each the boundary vertex  $q_j$  and  $\frac{1}{2}(|p_i|^2-1)$  for each interior vertex  $p_i$ . Fig. 3 shows the Brenier potential for the traditional optimal transportation map in the left frame, and the Pogorelov potential in the right frame. From the figure, we can see that the boundary value (the height) of the Brenier potential for the OT map has changes prominently, while the boundary of the Pogorelov potential is fixed with zero height.

We numerically verified whether the solutions to the Pogorelov problem satisfy the discrete Alexandrov

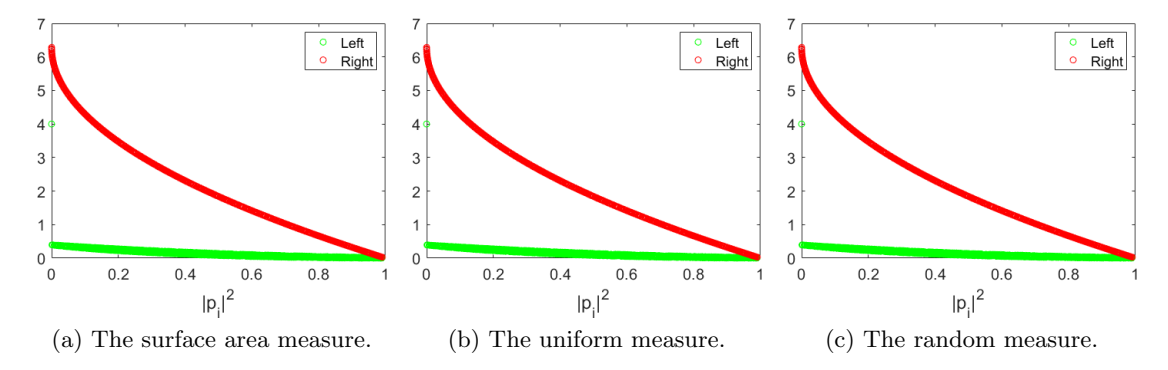


Figure 4: The verification of the Alexdrov maximum principle with different target measures.

maximum principle, the testing results are reported in Fig. 4. In the experiment, we randomly sample 15,000 points within the convex hull of  $\Omega^*$  and compute their corresponding u-values. The horizontal axis is the squared Euclidean distance from the sample point  $p_i$  to the origin, namely  $|p_i|^2$ . The green curve shows the graph of the function of  $|u(p_i)|^2$ , namely the left hand side of the inequality of Eqn. (8). The red curve shows the graph of the function defined by the right hand side of Eqn. (8), where the dimensional constant  $c_2 = 1$ , the diameter of  $\Omega$  is  $diam(\Omega) = 2$ , the total target measure  $|\partial u(\Omega)| = \pi$  for our experiments. It is obvious that the red curve is above the green curve, and their difference monotonously decreases. This shows that the discrete Alexandrov maximum principle holds.

# 5.4 Measure Preserving Property of Pogorelov Maps

In this part, we show that the solution to the Pogorelov problem induces a measure preserving map. For the male model shown in Fig. 5(a) and its conformal mapping image in Fig. 5(b), we define the target measure as in the case 1 of Sec. 5.2. Fig. 5(c) shows the result of optimal transportation map using the method in [2]. Fig. 5(d) shows the Pogorelov map using our proposed algorithm.

Fig. 6 shows the histogram of the area distortion factors for the interior vertices in different iterations. For each interior vertex  $v_i \notin \partial S$ , the area distortion factor is defined as

$$\log \mu(W_i(\mathbf{h})) - \log \nu_i, \quad i \in \{1, 2, \dots, n\}.$$

From the histograms, it is obvious that the proposed algorithm converges very fast, and for nearly all the interior vertices, the area distortion factor is close to zero, namely  $\mu(W_i(\mathbf{h}))$  is close to  $\nu_i$  and the histogram looks like a Dirac function concentrated at the origin. This shows that the Pogorelov mapping are measure-preserving, and has the potential to replace optimal transportation maps for practical applications due to

its efficiency and simplicity.

To measure the running time of the proposed method, we define the relative error to be

$$\varepsilon_i := |\mu(W_i) - \nu_i|/\nu_i$$

and set the maximum relative error tolerance as 1e-8 in Alg. 1. We report the number of the iterations for convergence, the corresponding running time, the total transportation cost of the OT map and the Pogorelov map, the root mean square erro (RMSE) between the OT map and the Pogorelov map in Tab. 1.

The first two rows show the results of the OT map with the second type boundary condition, the third and the forth rows demonstrate the results of the Pogorelov map with the Dirichlet boundary condition. In the first column, the target measure is the surface area measure defined in case 1 in subsection 5.2; in the second column, the target measure is the uniform measure defined in case 2; in the last three columns, the target measures are the random measure defined in case 3. From the table, we can see that Pogorelov map algorithm converges much faster than the optimal transportation map algorithm with slightly greater total transportation cost. Additionally, the root mean square error (RMSE) between the Pogorelov map and the OT map is very small.

Furthermore, by testing the Alexandrov maximum principle in the damping process, the robustness is greatly improved. Especially, when the temporary solution is close to the boundary of the admissible space, the original algorithm without maximum principle testing causes big fluctuations and become unstable. By adding the testing, the damping process is stabler and converges faster.

#### 6. CONCLUSION

In this work, we introduce a practical algorithm to solve the classical Pogorelov problem, and propose to

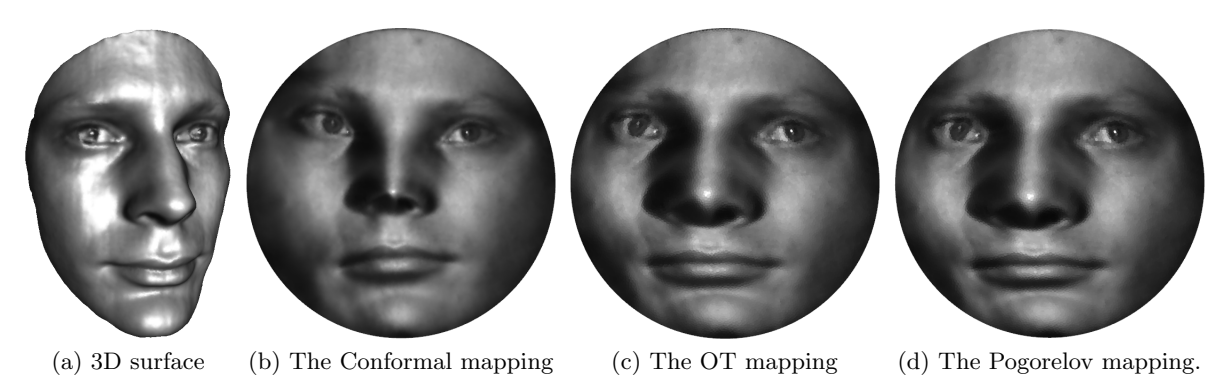


Figure 5: The results of the Alex model.

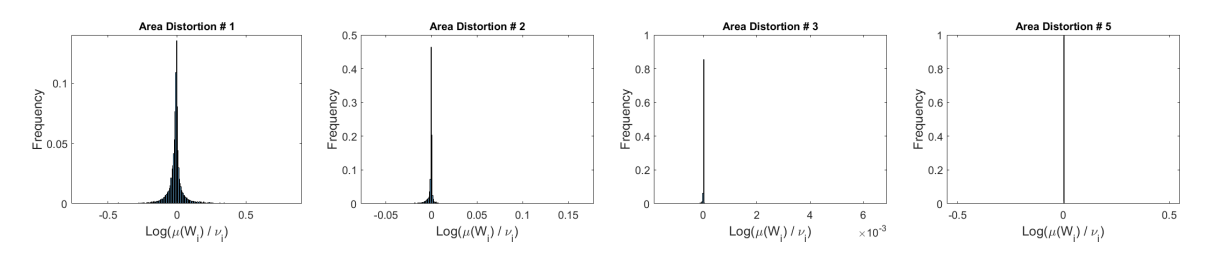


Figure 6: The histogram of the area distortion of the male facial model in different iterations.

use the measure-preserving Pogorelov map to approximate the optimal transportation map, due to its simplicity and efficiency. We also prove a discrete version of the classical Alexandrov maximum principle, which gives an apriori estimate for the solution to the Monge-Ampère equation with Dirichlet boundary condition.

Our experimental results demonstrate the efficiency and accuracy of the Pogorelov map, and verify the discrete Alexandrov maximum principle. Furthermore, the experiments also show that the robustness of the proposed algorithm can be improved by adding maximum principle testing.

In the future, we plan to generalize the algorithm to other geometric problems related to the Monge-Ampère equation, and use more apriori estimates on the discrete settings to further improve the efficiency and accuracy of the proposed algorithms.

Acknowledgement This research was partially supported by the Science Challenge Project of China (TZZT2019-B1), the National Natural Science Foundation of China (61720106005, 61772105, 61936002), NSF CMMI-1762287 collaborative research: computational framework fordesigning conformal stretchable electronics, and NSF DMS-1737812 collaborative research: ATD:theory and algorithms for discrete curvatures on network data from human mobility and monitoring.

#### References

- Zhao X., Su Z., Gu X., Kaufman A. "Area-Preservation Mapping using Optimal Mass Transport." *IEEE Transactions on Visualization and* Computer Graphics., vol. 19, no. 12, 2838 – 2847, 2013
- [2] Su Z., Wang Y., Shi R., Zeng W., Sun J., Luo F., Gu X. "Optimal Mass Transport for Shape Matching and Comparison." Pattern Analysis and Machine Intelligence, IEEE Transactions on, vol. 37, no. 11, 2246–2259, 2015
- [3] Haker S., Zhu L., Tannenbaum A., Angenent S. "Optimal mass transport for registration and warping." *International Journal of computer vi*sion, vol. 60, no. 3, 225–240, 2004
- [4] Arjovsky M., Chintala S., Bottou L. "Wasserstein generative adversarial networks." Proceedings of the 34th International Conference on Machine Learning-Volume 70, pp. 214–223. 2017
- [5] Wang X.J. "On the design of a reflector antenna II." Calculus of Variations and Partial Differential Equations, vol. 20, no. 3, 329–341, 2004
- [6] Wang X.J. "On the design of a reflector antenna." Inverse problems, vol. 12, no. 3, 351, 1996
- [7] Brenier Y. "Polar Factorization and Monotone Rearrangement of Vector-Valued Functions." Communications on Pure and Applied Mathematics, vol. 44, no. 4, 375–417, 1991

c 1. Comparison between the Optimal Transportation Map and the Logorciov							
		Iterations	8	13	12	13	13
-	ОТ	Time(s)	3.142	4.851	4.43	4.537	4.961
		Cost	0.0697	0.0671	0.0889	0.0666	0.0745
	Pogorelov	Iterations	5	12	10	12	11
		Time(s)	1.705	4.143	3.495	4.201	3.768
		Cost	0.0701	0.0674	0.0893	0.0674	0.0754
		RMSE	0.0313	0.0285	0.0150	0.0386	0.0167

Table 1: Comparison between the Optimal Transportation Map and the Pogorelov Map.

- [8] Gu X., Luo F., Sun J., Yau S.T. "Variational principles for Minkowski type problems, discrete optimal transport, and discrete Monge–Ampère equations." Asian Journal of Mathematics, vol. 20, no. 2, 383–398, 2016
- [9] Villani C. Topics in optimal transportation. 58. American Mathematical Soc., 2003
- [10] Villani C. Optimal transport: old and new, vol. 338. Springer Science & Business Media, 2008
- [11] Peyré G., Cuturi M., et al. "Computational Optimal Transport: With Applications to Data Science." Foundations and Trends® in Machine Learning, vol. 11, no. 5-6, 355-607, 2019
- [12] Monge G. "Mémoire sur la théorie des déblais et des remblais." Histoire de l'Académie Royale des Sciences de Paris, 1781
- [13] Kantorovich L. "On a problem of Monge." Uspekhi Mat. Nauk., vol. 3, 225–226, 1948
- [14] Kantorovich L.V. "On a problem of Monge." Journal of Mathematical Sciences, vol. 133, no. 4, 1383–1383, 2006
- [15] Benamou J.D., Brenier Y. "A computational fluid mechanics solution to the Monge-Kantorovich mass transfer problem." *Numerische Mathematik*, vol. 84, no. 3, 375–393, 2000
- [16] Santambrogio F. "Optimal transport for applied mathematicians." *Birkäuser*, NY, vol. 55, no. 58-63, 94, 2015
- [17] De Goes F., Cohen-Steiner D., Alliez P., Desbrun M. "An optimal transport approach to robust reconstruction and simplification of 2d shapes." *Computer Graphics Forum*, vol. 30, pp. 1593– 1602. Wiley Online Library, 2011
- [18] Cuturi M. "Sinkhorn distances: Lightspeed computation of optimal transport." Advances in neural information processing systems, pp. 2292– 2300. 2013

- [19] Solomon J., Rustamov R., Guibas L., Butscher A. "Earth mover's distances on discrete surfaces." ACM Transactions on Graphics (TOG), vol. 33, no. 4, 67, 2014
- [20] Solomon J., De Goes F., Peyré G., Cuturi M., Butscher A., Nguyen A., Du T., Guibas L. "Convolutional Wasserstein distances: Efficient optimal transportation on geometric domains." ACM Transactions on Graphics (TOG), vol. 34, no. 4, 66, 2015
- [21] Aurenhammer F. "Power diagrams: properties, algorithms and applications." SIAM Journal on Computing, vol. 16, no. 1, 78–96, 1987
- [22] De Goes F., Breeden K., Ostromoukhov V., Desbrun M. "Blue noise through optimal transport." ACM Transactions on Graphics (TOG), vol. 31, no. 6, 171, 2012
- [23] Lévy B., Schwindt E.L. "Notions of optimal transport theory and how to implement them on a computer." Computers & Graphics, vol. 72, 135– 148, 2018
- [24] Mérigot Q. "A multiscale approach to optimal transport." Computer Graphics Forum, vol. 30, pp. 1583–1592. Wiley Online Library, 2011
- [25] Cui L., Qi X., Wen C., Lei N., Li X., Zhang M., Gu X. "Spherical optimal transportation." Computer-Aided Design, vol. 115, 181–193, 2019
- [26] Benamou J., Brenier Y., Guittet K. "The Monge-Kantorovitch mass transfer and its computational fluid mechanics formulation." *International Jour*nal for Numerical Methods in Fluids, 2002
- [27] Su K., Cui L., Qian K., Lei N., Zhang J., Zhang M., Gu X.D. "Area-preserving mesh parameterization for poly-annulus surfaces based on optimal mass transportation." Computer Aided Geometric Design, vol. 46, 76–91, 2016
- [28] Su K., Chen W., Lei N., Zhang J., Qian K., Gu X. "Volume preserving mesh parameterization based on optimal mass transportation." Computer-Aided Design, vol. 82, 42–56, 2017

- [29] Dominitz A., Tannenbaum A. "Texture mapping via optimal mass transport." Visualization and Computer Graphics, IEEE Transactions on, vol. 16, no. 3, 419–433, 2010
- [30] ur Rehman T., Haber E., Pryor G., Melonakos J., Tannenbaum A. "3D nonrigid registration via optimal mass transport on the GPU." *Medical* image analysis, vol. 13, no. 6, 931–940, 2009
- [31] Su Z., Zeng W., Shi R., Wang Y., Sun J., Gu X. "Area preserving brain mapping." Proceedings of the IEEE Conference on Computer Vision and Pattern Recognition, pp. 2235–2242. 2013
- [32] Nadeem S., Su Z., Zeng W., Kaufman A.E., Gu X. "Spherical Parameterization Balancing Angle and Area Distortions." *IEEE Trans. Vis. Comput. Graph.*, vol. 23, no. 6, 1663–1676, 2017
- [33] Guan P., Wang X.J., et al. "On a Monge-Ampere equation arising in geometric optics." J. Diff. Geom, vol. 48, no. 48, 205–223, 1998
- [34] Gutiérrez C.E., Huang Q. "The refractor problem in reshaping light beams." Archive for rational mechanics and analysis, vol. 193, no. 2, 423–443, 2009
- [35] Meyron J., Mérigot Q., Thibert B. "Light in power: a general and parameter-free algorithm for caustic design." SIGGRAPH Asia 2018 Technical Papers, p. 224. ACM, 2018
- [36] Courty N., Flamary R., Tuia D., Rakotomamonjy A. "Optimal transport for domain adaptation." *IEEE transactions on pattern analysis and ma*chine intelligence, vol. 39, no. 9, 1853–1865, 2016
- [37] Chizat L., Bach F. "On the global convergence of gradient descent for over-parameterized models using optimal transport." Advances in neural information processing systems, pp. 3036–3046. 2018
- [38] Kandasamy K., Neiswanger W., Schneider J., Poczos B., Xing E.P. "Neural architecture search with bayesian optimisation and optimal transport." Advances in neural information processing systems, pp. 2016–2025. 2018
- [39] Genevay A., Peyré G., Cuturi M. "Learning generative models with sinkhorn divergences." *International Conference on Artificial Intelligence and Statistics*, pp. 1608–1617. 2018
- [40] An D., Guo Y., Lei N., Luo Z., Yau S.T., Gu X. "AE-OT: A new generative model based on extended semi-discrete optimal transport." International Conference on Learning Representations. 2019

- [41] An D., Guo Y., Zhang M., Qi X., Lei N., Gu X. "AE-OT-GAN: Training GANs from data specific latent distribution." *European Conference on Computer Vision (ECCV)*, p. 548–564. 2020
- [42] Alexandrov A.D. Convex polyhedra. Springer Science & Business Media, 2005
- [43] Gu X., Luo F., Sun J., Yau S.T. "Variational principles for Minkowski type problems, discrete optimal transport, and discrete Monge-Ampere equations." arXiv preprint arXiv:1302.5472, 2013
- [44] Berg M.d., Cheong O., Kreveld M.v., Overmars M. Computational Geometry: Algorithms and Applications. Springer-Verlag TELOS, Santa Clara, CA, USA, 3rd ed. edn., 2008
- [45] Lawson C.L. "Transforming triangulations." Discrete Mathematics, 1972
- [46] Guennebaud G., Jacob B., et al. "Eigen v3." http://eigen.tuxfamily.org, 2010
- [47] Zeng W., Samaras D., Gu D. "Ricci Flow for 3D Shape Analysis." *IEEE Trans. Pattern Anal.* Mach. Intell., vol. 32, no. 4, 662–677, Apr. 2010